Evolution of physical properties with decreasing size in $Ce(Ru_{0.4}Rh_{0.6})_2Si_2$

J. S. Kim and G. R. Stewart
Department of Physics, University of Florida, Gainesville, Florida 32611-8440, USA

K. Samwer
I Physikalisches Institut, Universität Göttingen, 37077 Göttingen, Germany

(Received 18 February 2009; revised manuscript received 30 March 2009; published 28 April 2009)

We have investigated the effect of size on the specific heat and magnetic susceptibility of heavy Fermion $Ce(Ru_{1-x}Rh_x)_2Si_2$ at $x=0.6$, which is a composition near a quantum critical point. Samples in the form of pellets pressed from powders ranging over two decades in size from $d\sim 0.6-1.2$ μm up to 53–120 μm were investigated. Size was characterized via sieving ($d>20$ μm) or filtration ($d\leq 20$ μm) through a series of decreasing size mesh or pores, by the line broadening of high-angle x-ray lines, as well as scanning electron microscopy measurements on the smallest particles. The magnetic susceptibility, χ, at low temperature increases strongly at the smallest sizes, reaching approximately a factor of 5 increase for the smallest powders vs the starting bulk material χ value. The magnitude and temperature dependence of the low-temperature specific heat, C, ($C/T\sim \log T$ at a quantum critical point) down to 0.15 K remains essentially unchanged with size reduction down to 3 μm. Below 3 μm, however, a new regime is entered. C/T at low temperatures begins to show a steep increase, i.e., it becomes more divergent, above the log T behavior, with $C/T\sim \gamma+aT^{-0.67}$ over more than two decades of temperature down to 0.1 K. This altered non-Fermi-liquid temperature dependence is consistent with the low-temperature behavior of χ and with the field dependence of the magnetization. Together, these emergent properties at the verge of the nanosize regime are reminiscent of Griffiths phase (rare spin cluster) behavior. Thus, decreasing the size down to ~ 1 μm does not reveal size limitation of the infinite-range fluctuations expected at this quantum critical point. Instead, strain and defects inherent in the small size appear to produce rare spin cluster-dominated effects as $d\rightarrow 1-3$ μm, with uncompensated local-moment defects becoming more dominant as size reaches the nanoregime $d\sim 0.6-1.2$ μm—consistent with the previous Kondo-dominated results on 20-nm-sized Ce compounds. Whether such rare spin cluster effects would also occur *away* from the quantum critical concentration is discussed.

DOI: 10.1103/PhysRevB.79.165119 PACS number(s): 71.10.Hf, 71.27.+a, 75.20.Hr, 75.50.Tt

I. INTRODUCTION

Strongly correlated electron materials have many interesting low-temperature properties, perhaps chief among them are the enhanced specific heat divided by temperature C/T and the enhanced magnetic susceptibility χ. A recently developed subfield for strongly correlated electron materials has been the unusual non-Fermi-liquid (nFl) behavior[1] observed in those systems which are close to a quantum critical point where a second-order phase transition, e.g., antiferromagnetism, has been suppressed just to $T=0$. Then, the *finite* temperature behavior can be dominated by quantum-mechanical fluctuations that are "infinite" (or at least very long range) in extent in space and time.

One unanswered question in this field is what happens to the fluctuations at a quantum critical point if the material is made smaller? Also, at what size will the ubiquitous Kondo effect seen in the previous[2–4] nanoparticle work on Ce compounds appear?

Technically, as will be discussed in Sec. II below, there are a number of challenges in pursuing these questions, chief among them is how to make the system smaller without introducing spurious magnetic contamination on the surface of the particles and therefore masking the intrinsic behavior of χ. Also, how to make a sequence of sizes that are intercomparable and reproducible was a further deciding criterion in the method chosen.

For the present work, we chose the $Ce(Ru_{1-x}Rh_x)_2Si_2$ system, where we discovered[5] quantum criticality at $x=0.6$, where C/T diverges as $T\rightarrow 0$ as log T, vs the behavior expected of a Fermi liquid where C/T approaches a constant as $T\rightarrow 0$. For the sizes discussed here, down to 0.6 μm, it is not expected[6] that the antiferromagnetic ordering temperature, T_N, will vary with size. Thus the concentration, $x=0.6$, where $T_N\rightarrow 0$ and where there is therefore a quantum critical point should stay constant.

The field of measuring the specific heat of a collection of small metal particles began in the 1970s with work on granular Al films[7] (~1 μm particles), Pb particles[8] (~30 Å) in porous glass, and Pt particles[9] (~10 Å) cosputtered with SiO_2. The first two works focused on phonon softening effects, while the Pt-particle work addressed the possibility of the discretization of electronic energy levels as the number of electrons in a collection of electrically isolated particles became small. Starting in the mid 1990s until the present there has been a resurgence of interest in size effects on metallic properties, using both improved preparation and characterization techniques. These seminal works on measuring χ and C in small particles include nano-Ce systems, including (Ce,Al) compounds and $CePt_2$,[2–4] as well as nanoparticles of Pd,[10] zinc ferrite,[11] and CdSe.[12] None of these systems is near a quantum critical point. In the nano-Ce compound particles, the specific-heat studies[2–4] (measured on ~20 mg pressed pellets of the powders) showed an enhancement of the number of Ce $4f$ ions contributing to a

low-temperature Kondo anomaly, which is a signature of uncompensated (by Kondo screening) Ce $4f$ magnetic moments. Presumably, the damage (lattice point defects or dislocations) in the neighborhood of the Ce ions caused by the production process was instrumental in causing this more magnetic behavior.

A number of preparation methods for these nano-Ce systems were used, but all resulted in very small (3–25 nm) sized particles, with no investigation of sizes between these and bulk material. The purpose of the present work is to investigate the evolution with decreasing size of the low-temperature electronic properties of quantum critical $Ce(Ru_{0.4}Rh_{0.6})_2Si_2$. Since any process by which particles are made smaller must carry some associated damage, the magnetic fluctuations present in our $Ce(Ru_{0.4}Rh_{0.6})_2Si_2$ system will in some size range begin to be affected by defects and strain introduced into the lattice. The level and type of damage that produced the observed[2–4] nano-Ce particle large Kondo contribution to χ and specific heat dominated the low-temperature magnetic and thermodynamic properties, with no results tracking the evolution of these properties at intermediate sizes.

In any case, we are not discussing the limit in which nanoparticles have different properties[9] due to discrete energy levels, since our particles (down to 600 nm in size) are both too large for this effect and still weakly electrically connected at the grain interfaces in the pressed pellets of powders used for this work. Thus, we report here on the evolution with decreasing size of the low-temperature magnetic susceptibility and specific heat of collections of $Ce(Ru_{0.4}Rh_{0.6})_2Si_2$ particles, where the bulk (and large grain) material shows typical quantum critical divergent behavior in C/T, which varies as $\log T$ down to 0.05 K. The particles have fairly narrow size distributions ranging from ~ 100 μm (showing bulk behavior) down to $\sim 0.6-1.2$ μm.

II. EXPERIMENTAL

A. Production of particles

Our design goals were to monotonically make succeeding decreases in particle size, to minimize contamination from magnetic elements such as Fe or Co, and to do the size reduction under liquid so that possible heat generation during the size reduction process would not cause uncontrolled annealing or chemical reactions such as oxidation. A further constraint was to have the process not require too large an amount of sample, since our materials are made in 1–2 g homogeneous arc-melted buttons from high-purity starting elements. The three processes investigated were ball milling (one of the processes used by Ho *et al.*[11] in their zinc ferrite work), grinding in a mortar under acetone, and rolling-mill processing. The primary techniques used by the nanoparticle works (flash evaporation[2–4,10] and laser ablation[3]) were not considered due to the small particle sizes inherent in these techniques and therefore a lack of continuity in tracking the properties of the material from the bulk.

Two ball mills that did not require large volumes of material, both from the company SPEX, were tried: the Model 8000 (capacity 130 ml), using zirconia container and balls, and the smaller Model 5100 (~ 15 ml capacity), using an agate vial and a single agate ball. Tungsten carbide, due to the large (magnetic) Co component, was not tried as a container material. Such ball mills shake the container vigorously, causing the ball(s) inside to impact the walls (and material to be milled) quite energetically. For the longer (>1 hr) periods necessary to pulverize the material small enough, it was found difficult in the ball mills tried to maintain the liquid sealed within. The loss of material smeared onto the walls and out the occasionally failed seal was significant.

We had significant initial success using rolling-mill techniques. The vessel chosen was Teflon (low contamination with magnetic impurities), the balls chosen were 10 mm diameter high-density (and strength) yttria-stabilized zirconia ($<0.01\%$ Fe_2O_3) from Glen Mills. The 185 ml Teflon vessel was approximately half filled with the zirconia balls, approximately 3 g of material to be ground [the material was either coarsely preground in an agate mortar under acetone to 230 mesh ($\Leftrightarrow 63$ μm) or introduced as mm-sized chunks], and then distilled water with two drops of Triton X-100 surfactant to impede clumping was added to the half full level. The speed of the rolling mill was adjusted to a rather slow level (~ 250 rpm) where good agitation of the balls was achieved at an approximate resonance mode frequency and allowed to run from one to three and a half weeks, which via experience produced ~ 5 mg of $0.6-1.2$ μm sized material and larger masses of larger sized material after the separation process. However, we discovered that—at least in the $Ce(Ru_{0.4}Rh_{0.6})_2Si_2$ being studied here—sufficient numbers of uncompensated magnetic Ce $4f$ electrons were introduced by the 10 μm size regime to totally mask any χ or C behavior from the majority of the Ce ions with undisturbed undamaged local moment-screening environments. Although such large uncompensated Ce-moment Kondo contributions were uniformly found in the Ce-nanoparticle work,[2–4] we wanted to delay such masking contributions to as low a size as possible in order to search for other possible effects associated with the quantum critical fluctuations in our system. This was one advantage of the present work's tracing the behavior of the particles with monotonically decreasing size.

A less damage-inducing method for producing fine powders was found to be simple grinding by hand in an agate mortar under acetone. Although this method is quite laborious for producing sufficient (~ 5 mg) amounts for characterization of particles below 10 μm in size, empirically it shifted the onset of significant low-temperature magnetic ion contributions to the specific heat to the $0.6-1.2$ μm regime, i.e., a factor of 10 smaller than the rolling-mill technique. Also, this method slowed the increase in χ at low temperature as well as the increase in the low-temperature saturation in M vs H, consistent with the presence of local moments, with decreasing particle size.

B. Separation of particles by size

For the larger sized particles (≥ 20 μm), the powders were dried followed by dry sieving through successively finer mesh screens. However, for sizes below 20 μm, due to

clumping (electrostatic cling), dry sieving did not produce sufficient quantities.

Separation of the smaller sizes was achieved by filtering particles suspended in water via ultrasonic agitation through successive sized Millipore "isopore" (straight holes) polycarbonate 47 mm diameter membrane filters on a fritted glass holder mounted into a large flask. The driving force for moving the liquid and particles through the micropore filters is supplied by pumping on the flask, thus sucking the water and particles that are smaller than the pore size of the filter into the flask. These techniques are common[13] in the carbon nanotube community (although smaller sized pores are typically used). The dried powder is scraped from the numerous (10–50 in number) filters used at each size gradation, collected, and either pressed as pellets for χ and specific-heat measurements or used for x-ray diffraction characterization.

We have developed a high-pressure $1/8''$ pellet press ($\sim$150 000 psi), suitable for mg quantities, which gives good thermal contact between the grains. (No significant grain growth under pressure was observed via, e.g., measurement of the high-angle x-ray line width.) This technique thus avoids serious pellet-internal thermal-conductivity problems (the τ_2 effect) in low-temperature specific-heat measurements.[14] In the dilution refrigerator used for measurements down to 0.1 K, our high-pressure pressed pellet samples had an additional advantage over, e.g., the representative data for a Cu sample presented in the apparatus paper,[14] i.e., the very large specific heat of this $Ce(Ru_{0.4}Rh_{0.6})_2Si_2$ material. Thus, we were able to use large ($\sim$1 mg) amounts of GE (General Electric) 7031 varnish to mount the pellets on the sapphire platform, further insuring excellent thermal contact between the grains without making the sample addenda too large. In fact, the total addenda correction to the specific heat for the samples reported here was always less than 3% below 1 K. Thus, the τ_2 correction to the specific heat due to inadequate thermal conductivity even down to 0.1 K for our samples was smaller than that shown in Ref. 14 for their Cu sample at 0.5 K.

Large numbers of filters are used, especially in the initial 10 μm pore-size filtration so that caking or blocking of the pores is minimized—allowing material that is smaller than the pore size to pass through. It should be noted however that some material that is smaller than the pore size will always be trapped (either due to pore blockage or clumping) above the filter. For the 10–20 μm size regime, the powder collected off the 10 μm micropore filters was reagitated and filtered again to reduce these effects. Thus, the powder size distributions quoted in the present work are nominal in the sense that a given range (e.g., 1.2–3 μm) will contain no material that is *larger* than the upper limit (e.g., 3 μm) of the range (since all the material collected on the 1.2 μm filter had to pass through the 3 μm filter first) but will most likely contain some material that is *smaller* than the stated lower limit (e.g., 1.2 μm) of the size range. Various checks and repetitions (e.g., χ was measured on powder of a certain size regime and then the source powder was subjected to an additional filtration pass than used for that sample and χ was remeasured) were performed to minimize this problem as far as possible. Figure 1 shows a scanning electron micrograph of material on a 0.6 μm pore-size Millipore filter. Although

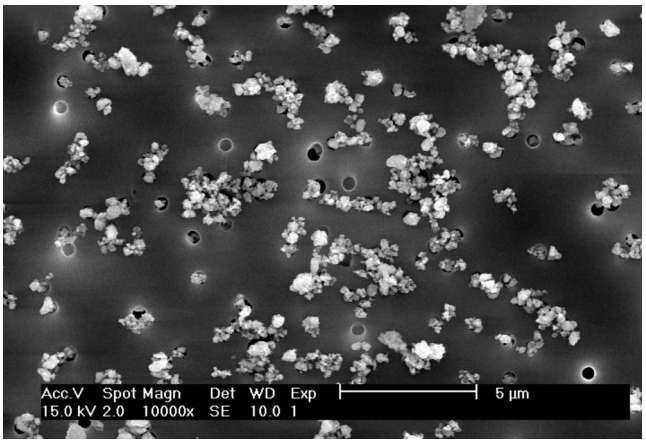

FIG. 1. A scanning electron micrograph of $Ce(Ru_{0.4}Rh_{0.6})_2Si_2$ powder on a 0.6 μm Millipore™ filter that has previously passed through a 1.2 μm filter. These and other SEM results helped to optimize the filtering process and reduce caking and clumping.

clumping has taken place on the filter (presumably during drying due to the surface tension of the water), this micrograph shows a relatively narrow size distribution without a large amount of material present that is smaller than 0.6 μm.

In addition to characterizing the size distribution by the pore size of the filter membranes and scanning electron microscopy (SEM) photographs (for $d<3$ μm), line widths of high-angle x-ray diffraction lines were also measured. Figure 2 shows the 97° 2θ line for 10–20 μm material prepared via rolling mill and via mortar grinding.

Clearly, the line widths shown here, which are affected by both size considerations and defects, indicate that the rolling-mill-produced material, for the same 10–20 μm size regime, has greater concentration of defects compared to the mortar-ground material. By the 1.2–3 μm size regime, the same 97° 2θ line for mortar and rolling-mill materials (see Fig. 3) is more similar in width, indicating a smaller differ-

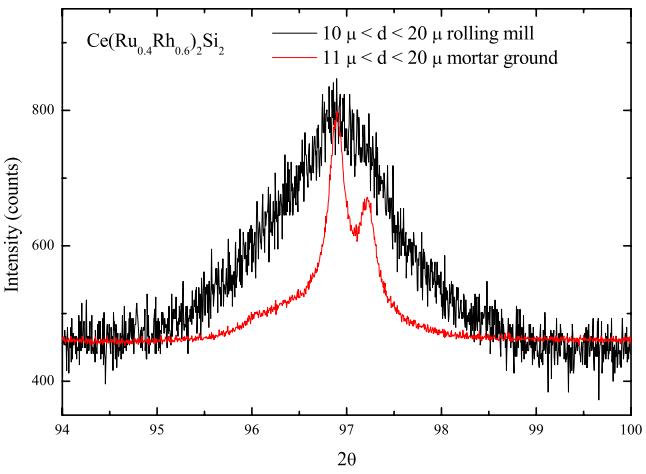

FIG. 2. (Color online) The full width at half maximum (FWHM)=0.77° 2θ for the rolling-mill material, i.e., half that for the 1.2–3 μm rolling-mill material shown below in Fig. 3. FWHM for the well-separated α_1-α_2 doublet lines at 97° 2θ for the mortar-ground material is about 0.16° 2θ, while the instrumental resolution of the diffractometer used is approximately 0.09° 2θ

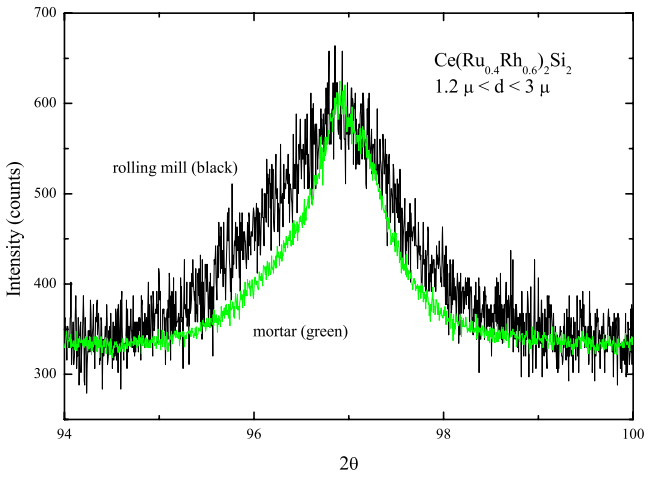

FIG. 3. (Color online) For the 97° 2θ peak, FWHM=1.53° 2θ for the rolling-mill material and 0.91° 2θ for the mortar material. These diffraction lines, although broad, are still well defined.

ence in the gross overall damage level from the two preparation techniques.

Since our work is focused on the evolution with decreasing size or increasing defect concentration on the electronic properties of quantum critical $Ce(Ru_{0.4}Rh_{0.6})_2Si_2$, the results discussed below will focus on the mortar-ground material. This process, among those investigated in this work, minimizes the effects on the measured properties of the unavoidable damage involved in producing particles of reduced size.

III. RESULTS AND DISCUSSION

A. Susceptibility and magnetization

The properties[5] of bulk, $Ce(Ru_{0.4}Rh_{0.6})_2Si_2$, including the low-temperature susceptibility and specific heat, are dominated by this composition being at a quantum critical point and its associated[1] nFl behavior. Figures 4 and 5 show how

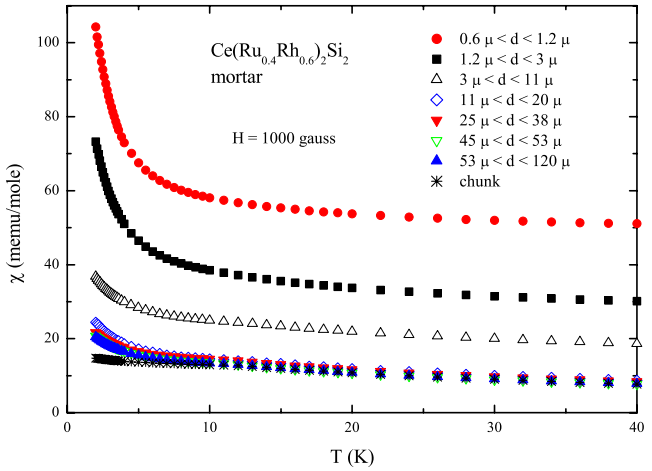

FIG. 4. (Color online) Low-temperature magnetic susceptibility of $Ce(Ru_{0.4}Rh_{0.6})_2Si_2$ as a function of decreasing size. The data below ~7 K for the chunk do not match the larger sized powder data due to some preferential orientation in the arc-melted button.

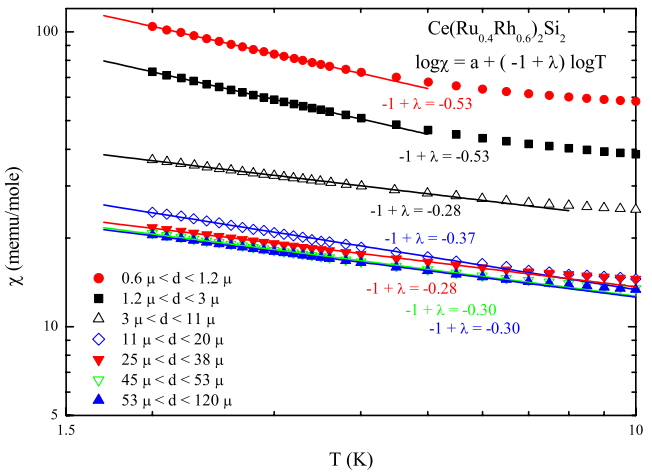

FIG. 5. (Color online) Logarithm of the low-temperature magnetic susceptibility χ of $Ce(Ru_{0.4}Rh_{0.6})_2Si_2$ as a function of size plotted vs log T. The slope of the data plotted in this fashion gives the exponent $(-1+\lambda)$ in $\chi=a+bT^{-1+\lambda}$, which changes from $\sim -0.32 \pm 0.04$ for the larger sizes to -0.53 for the two smallest sizes, 1.2–3 μm and 0.6–1.2 μm.

the low-temperature magnetic susceptibility, χ, of $Ce(Ru_{0.4}Rh_{0.6})_2Si_2$ varies from the nFl bulk behavior as a function of decreasing size.

The data in Fig. 4 show that the magnitude of χ at low temperatures for $Ce(Ru_{0.4}Rh_{0.6})_2Si_2$ remains essentially independent of size [$\chi(2\ \mathrm{K}) \sim 20-25$ memu/mole] down to 11 μm. At smaller sizes, the low-temperature magnitude of χ starts to increase substantially with decreasing size, i.e., qualitatively the material shows a tendency toward more magnetic behavior. The log χ vs log T data in Fig. 5 show a similar lack of change in the low-temperature dependence but down to the 3 μm size. The exponent in $\chi \sim T^{-1+\lambda}$ stays constant at about -0.3 down to and including the 3–10 μm size regime where Figs. 4 and 5 show that χ (2 K) has already risen from the bulk, ~20–25 memu/mole, value by 70%.

For the two smallest size regimes (1.2–3 μm and 0.6–1.2 μm) studied in the present work, the temperature dependence at our lowest measured temperature as shown in Fig. 5 changes, as is obvious visually. The change is from the $T^{-0.3}$ observed for $d > 1.2$ μm to $T^{-0.5}$. Since this inverse square-root temperature dependence is far from the Curie-Weiss behavior of $\chi \sim 1/T$, there do not appear to be uncompensated local moments present in measurable concentrations down to 2 K in these 0.6–1.2 μm and 1.2–3 μm particles. When the measurements of the low-temperature specific heat (which are sensitive to local moments in the 1%–2% range due to the associated entropy) are discussed below, this issue will be revisited. A contribution to the entropy ($\Leftrightarrow$bump in specific heat) from any such local moments is a more sensitive probe for the presence of local moments.

Another useful method for checking for the changes in magnetic behavior in a material is to measure the magnetization as a function of field. If the magnetization shows a tendency toward saturation at higher fields, this can be caused by a variety of effects. Combined with measurements

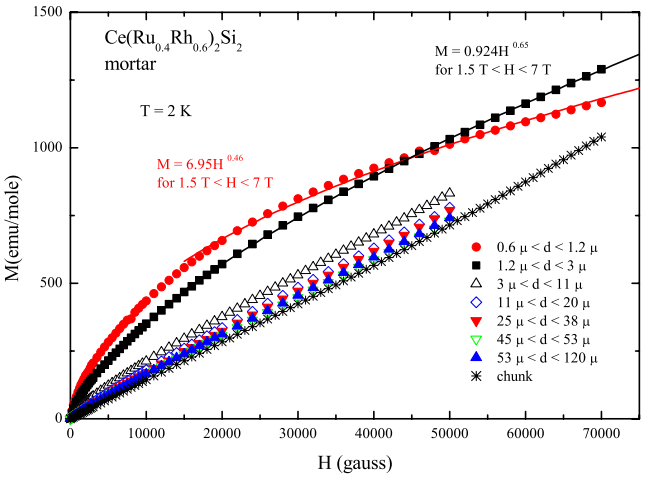

FIG. 6. (Color online) Magnetization vs field for $Ce(Ru_{0.4}Rh_{0.6})_2Si_2$ as a function of size up to 5 T (7 T for the two smallest sizes and the chunk). The fits of the data for the smallest sizes to the form $M \sim H^{\lambda}$ work well over the 1.5–7 T field range.

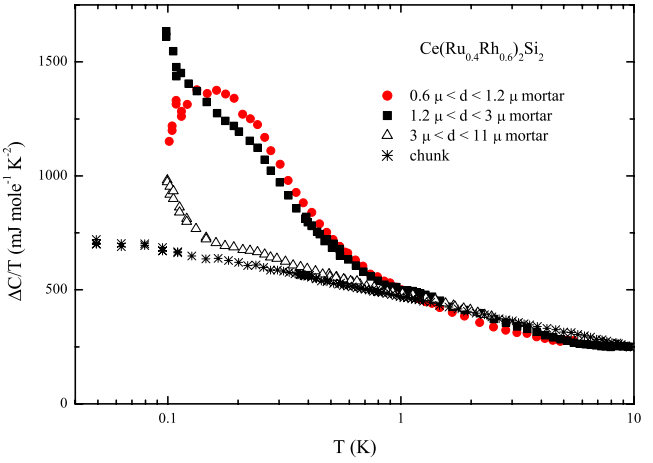

FIG. 7. (Color online) Specific heat, C, divided by temperature, T, for $Ce(Ru_{0.4}Rh_{0.6})_2Si_2$ as a function size vs log T. The specific heats for the size ranges 11–20 μm through 53–120 μm are very similar to the data shown for the bulk material and are not shown for clarity.

of χ and specific heat, magnetization measurements can help determine the cause of any increased magnetic behavior. If local moments are present at the temperature where M vs H is being measured, for instance due to noncompensated Ce moments in $Ce(Ru_{0.4}Rh_{0.6})_2Si_2$ due to lattice damage interrupting the Kondo compensation process, then—in addition to $\chi \sim 1/T$, the Curie-Weiss temperature dependence—the magnetization will show a tendency toward saturation as the increasing field aligns the local moments. In addition to this simple possible explanation for saturation in M vs H, there are also theories[1,15] and experiments[16,17] for non-Fermi-liquid systems with disorder that suggest that at higher fields the magnetization will vary as $M \sim H^{\lambda}$ where λ is the same parameter as in $\chi \sim T^{-1+\lambda}$. Figure 6 shows the M vs H data at 2 K measured on the various size regimes prepared via mortar grinding of $Ce(Ru_{0.4}Rh_{0.6})_2Si_2$. Just as in Fig. 5, where there is a change in the temperature dependence of the low temperature χ with decreasing size, Fig. 6 shows a definite increase in the saturation of the magnetization with increasing field for the same sizes where χ (2 K) grows so rapidly and where the low-temperature dependence, $T^{-1+\lambda}$, starts to change: 0.6–1.2 μm and 1.2–3 μm. It is worth noting that there is essentially no tendency toward saturation up to 5 T for the 3–11 μm particles, which showed in Fig. 4 a 70% increase in χ (2 K) vs the bulk value but showed the same temperature dependence at low temperature for χ in Fig. 5.

Figure 6 shows a fit to the M vs H field dependence extended to 7 T for the two smallest sized particles that show a tendency toward saturation. Note that the data can indeed be fitted to the rare spin cluster Griffiths phase theory[15] which predicts $M \sim H^{\lambda}$, and that the values for λ obtained (0.65 for 1.2–3 μm, 0.46 for 0.6–1.2 μm) are not inconsistent with the value for λ (0.47) obtained from the low-temperature dependence of χ for both sizes. The temperature and field dependence of the specific heat, discussed below, will help[16,17] further determine the applicability of this theory.

B. Specific heat

The progression with size of specific heat for $Ce(Ru_{0.4}Rh_{0.6})_2Si_2$ is shown in Fig. 7. Particles with size down to and including 11–20 μm show very similar behavior down to 0.3 K to that of the bulk nFl temperature dependence, i.e., $C/T \sim \log T$. The 3–11 μm particle specific heat shown in Fig. 7 follows $C/T \sim \log T$ down to 0.15 K where an upturn in C/T begins which appears to parallel the upturns in the C/T for 0.6–1.2 μm and 1.2–3 μm materials that begin at ~1 K. Thus, this upturn in the 3–11 μm C/T data is consistent with the same behavior seen in the 0.6–1.2 and 1.2–3 μm data but shifted to lower temperatures.

We consider now the specific-heat data for the 0.6–1.2 μm and 1.2–3 μm sizes shown in Fig. 7, which as discussed above show a different χ (2 K), a different temperature dependence in χ down to 2 K, and a distinctly different M vs H behavior than the larger sized particles. As may be seen in Fig. 7, the specific heat for these two smallest size regimes studied in the present work have C/T rising much more rapidly than for the bulk and larger sizes with decreasing temperature below 1 K. Above 1 K the C/T data for the small sizes show a slight minimum when plotted vs log T as in Fig. 7, rather than the $C/T \sim \log T$ straight-line behavior on such a plot shown by the 3–11 μm data and larger.

Considering first the C/T data for the 0.6–1.2 μm particles in Fig. 7, these data show a peak at around 0.17 K that is consistent with a small Kondo peak[18–20] or with a small Schottky anomaly due to magnetic impurities caused by the grinding process. This anomaly in the specific heat is imposed on a background that above 1 K is very similar to the bulk behavior. The entropy associated with the peak in these data is consistent with a small number (of the order of 5% of the Ce in the lattice) of magnetic spins. With the additional damage in this size range present in rolling-mill material, this peak is much more pronounced, and the approximate $C/T \sim \log T$ behavior above 1 K characteristic of the larger sizes is totally absent, see Fig. 8.

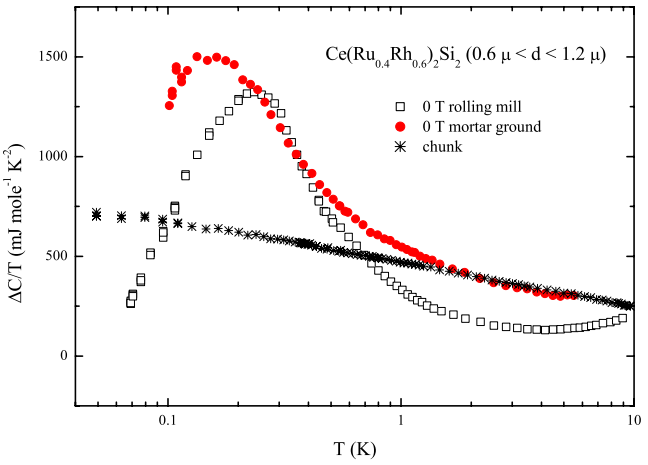

FIG. 8. (Color online) $\Delta C/T$ vs log T for $Ce(Ru_{0.4}Rh_{0.6})_2Si_2$ for 0.6–1.2 μm particles prepared with both the rolling mill and the mortar techniques compared to bulk material. ΔC has the lattice contribution subtracted. The amount of entropy under the rolling-mill data corresponds to ~20% of Ce $4f$ $S=1/2$ spins. The peak in the rolling-mill data (proportional to the level splitting, T_0, or Kondo temperature, T_K) is shifted upward in the temperature vs the mortar-ground material. Also, $\chi \sim 1/T$ at low temperatures (not shown) for the rolling-mill material, i.e., χ is dominated by the Curie-Weiss local-moment behavior. Results (not shown) for rolling-mill-produced particles of $Ce(Ru_{0.7}Rh_{0.3})_2Si_2$ showed similar behavior to that shown here for the rolling-mill $x=0.6$ material, i.e., at least the tendency of $Ce(Ru_{0.4}Rh_{0.6})_2Si_2$ with higher concentrations of defects to have this peak in C/T is *not* a function of nearness to a quantum critical transition.

The specific heat in 0, 1, and 2 T for 0.6–1.2 μm mortar-ground particles is shown in Fig. 9. These data are qualitatively similar with zero and applied field data from the Ce-nanoparticle works,[2,3] where the data were analyzed as having large Kondo contributions. The nanoparticle Ce work, e.g., for[3] 3.1–26 nm $CePt_2$ particles, sees much larger peak

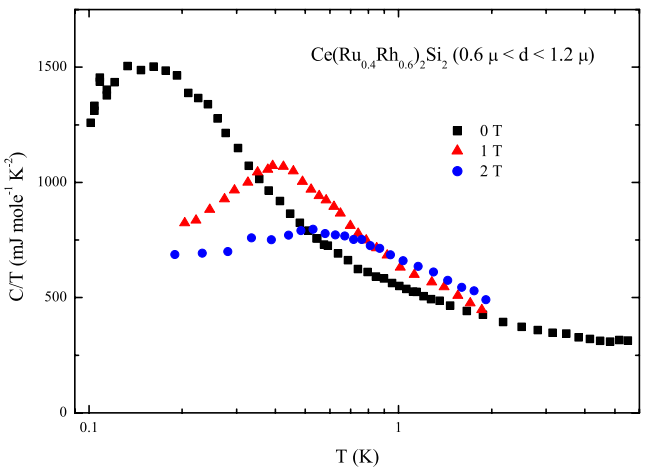

FIG. 9. (Color online) Peak in C/T for mortar-ground $Ce(Ru_{0.4}Rh_{0.6})_2Si_2$ moves up in T with increasing field, broadens, and gets smaller. The field dependence shown may also be describable by rare spin clusters (Refs. 15–17) in addition to that by the Kondo effect.

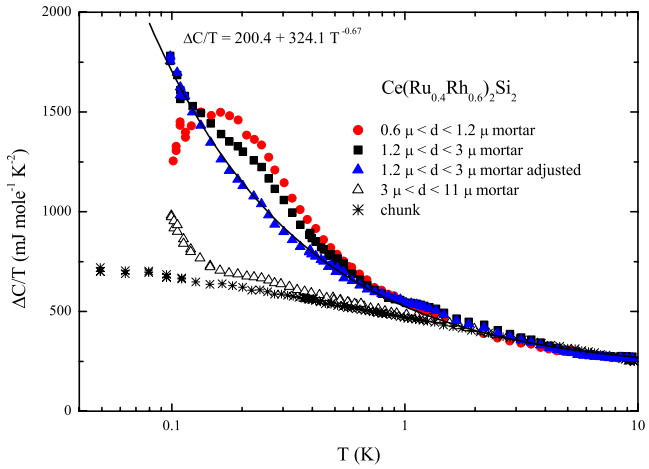

FIG. 10. (Color online) Low-temperature C/T data with the lattice contribution subtracted vs log T for $Ce(Ru_{0.4}Rh_{0.6})_2Si_2$. The data for 1.2–3 μm particles adjusted by the subtraction of a small magnetic impurity or Kondo peak, shown by the solid triangles, agree with unadjusted data (squares) above about 0.7 K and below 0.13 K, i.e., the influence of this peak is slightly outside of a narrow temperature range. It is likely that this same upturn behavior exists in the 0.6–1.2 μm data as well, since Fig. 8 makes clear that the mortar material has a relatively small contribution from uncompensated magnetic spins compared with the rolling-mill material. However, the more dominant peak in the 0.6–1.2 μm material vs that in the 1.2–3 μm makes it difficult to cleanly separate and analyze the contributions.

sizes, consistent with (of the order of 25%–50%) Ce $4f$ $S=1/2$ spins, with the peak temperature varying between 0.3 and 2 K. Similarly, the results[2] for 8 nm $CeAl_2$ are fit well via the Kondo theory,[20] with approximately 30% of the Ce spins contributing to the Kondo peak. Thus, the previous work on small particles of Ce compounds in the nanosized regime showed already low-temperature specific-heat behavior dominated by peaks in C/T due to 25%–30% of uncompensated local Ce $4f$ moments.

Our $Ce(Ru_{0.4}Rh_{0.6})_2Si_2$, as it enters into the nanoregime for our 0.6–1.2 μm particles (Fig. 7), has the specific heat beginning to be dominated by the low-temperature peak from only ~5% of the uncompensated Ce $4f$ local-moment spins. If we calculate the Wilson ratio $[R=218.7\chi(T \rightarrow 0)/\mu_{\text{eff}}^2\gamma$, with χ in units of memu/mole, γ in units of mJ/mol K^2, and μ_{eff} in units of Bohr magneton $\mu_B]$ for this size, using $\mu_{\text{eff}}=2.54\mu_B$ for Ce $4f^1$ and χ and C/T values from 2 K, we obtain ~9.5, compared to 1.9 for the quantum critical, near a magnetic instability, bulk material. Thus there is a large increase in the magnetic behavior of $Ce(Ru_{0.4}Rh_{0.6})_2Si_2$ upon reduction in size to the ~1 μm regime.

The one size in the present work where we can analyze the low-temperature specific-heat data that have evolved from the bulk behavior with decreasing size but are not yet dominated by a low-temperature peak is our 1.2–3 μm sample shown above in Fig. 7 and reanalyzed in Fig. 10. Here, the incipient peak corresponds to only about 0.7% of Ce $4f$ $S=1/2$ spins vs the ~5% present in the 0.6–1.2 μm particle mortar-ground data. For analyzing temperature de-

pendences from the fluctuations characteristic of the majority of the Ce spins, this is a much more tractable level of magnetic defects. Figure 10 shows the 1.2–3 μm data with the slight bulge, along with a plot of these data with a fit to the minor anomaly subtracted. The adjusted C/T data can be fitted over two decades of temperature to $C/T=a+bT^{-0.67}$. If this exponent is set equal to $-1+\lambda$, then $\lambda=0.33$. This may be compared to $\chi\sim T^{-0.53}$ (Fig. 5) ($\lambda=0.47$) and $M\sim H^{\lambda}$, with $\lambda=0.65$ (Fig. 6). These values for λ show a disagreement larger than that observed in work[17] $Ce_{1-x}Th_xRhSb$ where the Griffiths phase theory was applied to specific heat and magnetic-susceptibility data, where the λ's ranged between 0.64 and 0.74. However, the present work's range of λ's is smaller than that observed in a Griffiths phase analysis[16] of $Ce_{1-x}La_xRhIn_5$. Certainly it is plausible that, as the size of $Ce(Ru_{0.4}Rh_{0.6})_2Si_2$ is reduced with the inherent increase in strain and defects in the lattice, the Griffiths phase behavior (rare spin clusters) could dominate. In any case, rather than the quantum critical fluctuations producing $C/T\sim\log T$, another divergent (power-law) behavior is observed, certainly for the 1.2–3 μm sized particles and—by inference—possibly also for the 0.6–1.2 μm sized particles. Whether this power-law behavior is tied to $Ce(Ru_{0.4}Rh_{0.6})_2Si_2$ being near a quantum critical point is an interesting question. One would think that, given the presence of Ce $4f$ ions and sufficient defects, rare spin clusters would not be dependent on the infinite-range fluctuations unique to the quantum critical concentration. In fact, in (bulk) $Ce_{0.05}La_{0.95}RhIn_5$ (Ref. 16) Griffiths phase behavior occurs *away* from a quantum critical point while in $Ce_{0.8}Th_{0.2}RhSb$ (Ref. 17) it occurs *at* a quantum critical point.

IV. CONCLUSIONS

The present work reports the evolution of χ, M vs H, and C/T with decreasing particle size for $Ce(Ru_{0.4}Rh_{0.6})_2Si_2$. Mortar grinding was chosen to minimize damage compared to either rolling mill or ball mill techniques. Size regimes between 0.6–1.2 μm and 53–120 μm were prepared and characterized, with essentially the bulk properties present down to the 11–20 μm size regime. Upon further size reduction, the low-temperature electronic properties of bulk $Ce(Ru_{0.4}Rh_{0.6})_2Si_2$ began to exhibit increasing divergence with decreasing temperature, with $\chi\sim T^{-0.53}$ and $C/T\sim T^{-0.67}$ dependences for the 1.2–3 μm particles—reminiscent of Griffiths phase behavior of rare spin clusters. Upon further reduction to the 0.6–1.2 μm size regime, the peak in the low-temperature specific heat previously observed in nanoparticles of several Ce compounds was present for about 5% of the Ce spins, making it difficult to further follow the evolution of the bulk behavior to lower sizes. If further reduction in the defect concentrations responsible for the uncompensated magnetic spins could be effected, e.g., by annealing the powders without chemical contamination from the large surface-to-volume ratios and exposure to surfactants during the size reduction and separation procedures, it would be interesting to follow the possible evolution in the behavior of the quantum critical fluctuations further into the nanoregime. Work on U systems, where damage has less tendency to produce uncompensated local-moment effects, and on $Ce(Ru_{1-x}Rh_x)_2Si_2$ away from a quantum critical point is underway.

ACKNOWLEDGMENTS

Work at Florida was carried out under the auspices of the U.S. Department of Energy under Contract No. DE-FG02-86ER45268. Work at Universitaet Goettingen was carried out under the auspices of the DFG Leibniz program and the SFB 602. Useful conversations with K. Ingersent, A. Rinzer, and P. Schlottmann as well as the technical assistance of Ute Bete, I Physikalisches Institut Universitaet Goettingen, and Wayne Acree, Valentin Craciun, and Eric Lambers, Major Analysis Instrumentation Center, University of Florida, are gratefully acknowledged.

[1] G. R. Stewart, Rev. Mod. Phys. **73**, 797 (2001); G. R. Stewart, *ibid.* **78**, 743 (2006); H. v. Löhneysen, A. Rosch, M. Vojta, and P. Woelfe, *ibid.* **79**, 1015 (2007).

[2] Y. Y. Chen, Y. D. Yao, C. R. Wang, W. H. Li, C. L. Chang, T. K. Lee, T. M. Hong, J. C. Ho, and S. F. Pan, Phys. Rev. Lett. **84**, 4990 (2000).

[3] Y. Y. Chen, P. H. Huang, M. N. Ou, C. R. Wang, Y. D. Yao, T. K. Lee, M. Y. Ho, J. M. Lawrence, and C. H. Booth, Phys. Rev. Lett. **98**, 157206 (2007).

[4] S. W. Han, C. H. Booth, E. D. Bauer, P. H. Huang, Y. Y. Chen, and J. M. Lawrence, Phys. Rev. Lett. **97**, 097204 (2006).

[5] J. S. Kim, D. J. Mixson, D. Burnette, B. Andraka, K. Ingersent, G. R. Stewart, E. W. Scheidt, and W. Scherer, Phys. Rev. B **74**, 165112 (2006).

[6] For example, 13 nm particles of Tb still display approximately the bulk magnetic ordering temperature, see D. Johnson, P. Perera, and M. J. O'Shea, J. Appl. Phys. **79**, 5299 (1996).

[7] R. L. Greene, C. N. King, R. B. Zubeck, and J. J. Hauser, Phys. Rev. B **6**, 3297 (1972).

[8] V. Novotny, P. P. Meincke, and J. H. Watson, Phys. Rev. Lett. **28**, 901 (1972); H. P. Baltes and E. R. Hilf, Solid State Commun. **12**, 369 (1973).

[9] G. R. Stewart, Phys. Rev. B **15**, 1143 (1977).

[10] Y. Y. Chen, Y. D. Yao, S. S. Hsiao, S. U. Jen, B. T. Lin, H. M. Lin, and C. Y. Tung, Phys. Rev. B **52**, 9364 (1995).

[11] J. C. Ho, H. H. Hamdeh, Y. Y. Chen, S. H. Lin, Y. D. Yao, R. J. Willey, and S. A. Oliver, Phys. Rev. B **52**, 10122 (1995).

[12] S. Neeleshwar, C. L. Chen, C. B. Tsai, Y. Y. Chen, C. C. Chen, S. G. Shyu, and M. S. Seehra, Phys. Rev. B **71**, 201307(R) (2005).

[13] A. Rinzler (personal communication).

[14] G. R. Stewart, Rev. Sci. Instrum. **54**, 1 (1983); H. Tsujii, B. Andraka, E. C. Palm, T. P. Murphy, and Y. Takano, Physica B **329-333**, 1638 (2003).

[15] A. H. Castro Neto, G. Castilla, and B. A. Jones, Phys. Rev. Lett. **81**, 3531 (1998); A. H. Castro Neto and B. A. Jones, Phys. Rev. B **62**, 14975 (2000).
[16] J. S. Kim, J. Alwood, D. Mixson, P. Watts, and G. R. Stewart, Phys. Rev. B **66**, 134418 (2002).
[17] J. S. Kim, E.-W. Scheidt, D. Mixson, B. Andraka, and G. R. Stewart, Phys. Rev. B **67**, 184401 (2003).
[18] P. D. Sacramento and P. Schlottmann, Phys. Rev. B **40**, 431 (1989).
[19] P. D. Sacramento and P. Schlottmann, Phys. Rev. B **42**, 743 (1990).
[20] P. D. Sacramento and P. Schlottmann, Phys. Rev. B **43**, 13294 (1991).